

# Understanding the Properties of Slags

Seshadri SEETHARAMAN,<sup>1,2)\*</sup> Lidong TENG,<sup>1)</sup> Miyuki HAYASHI<sup>3)</sup> and Lijun WANG<sup>4)</sup>

1) Division of Materials Process Science, Royal Institute of Technology, Stockholm, SE-100 44 Sweden.

2) TU Bergakademie, Freiberg, D-09599 Germany.

3) Tokyo Institute of Technology, Tokyo, 152-8552 Japan.

4) University of Science and Technology Beijing, Beijing, 100083 China.

(Based on Honorary Member lecture; manuscript received on May 14, 2012; accepted on August 27, 2012)

Understanding of the properties of slags is a pre-requisite in optimizing their functions towards the making and refining of steel. Important contributions towards this objective have been made over the past half a century, in different parts of the world, especially in USA, UK, Germany and most of all in Japan. Knowledge of the slag properties enables in understanding the slag structure as well. The present review paper summarizes the contributions made in this field by the Division of Materials Process Science, Royal Institute of Technology, Stockholm, Sweden.

The paper deals with the measurement and modeling of (a) thermochemical properties of slags, (b) thermophysical properties and (c) inter-property correlations. Some important contributions during recent years, such as the determination of the valence states of Cr and V in slags, wetting characteristics related to hot-metal desulphurization, diffusion of sulphide ions in slags, partition of phosphorus between slag and metal phases and studies on process phenomena such as foaming are highlighted. The research work has led to the evolution of a new basicity concept. Dynamic physical property measurements are pointed out to be an experimental tool towards understanding of reaction mechanisms. Developments with respect to slag/metal interfacial phenomena, viz. the concept of surface velocity and surface viscosity and quantification of these properties are presented.

**KEY WORDS:** slags; steelmaking; thermochemistry; slag capacities; thermophysics; viscosities; refining; process phenomena; interfacial phenomena.

## 1. Introduction

It is well-known that slags play an important role in metals production and refining. Despite the importance of its function, slags have always remained a mystery to metallurgists. This is specially true in the case of steel metallurgy as slag properties have to be understood and solved for optimizing the science and technology of iron- and steelmaking. Intensive research has been going on in different parts of the world, especially in the industrialized countries to understand the properties of slag and utilize the same for improving the steelmaking processes. Special mention should be made of the great advances made in slag research in the 50's, 60's and 70's in the USA by the legendary scientists like Professor Chipman, Professor Elliott and Professor Darken, in the UK, by Professor Richardson and Professor Bell and in Germany, by Professor Schenck. Already in the 60's, Japan had taken a leading role in studying the slag properties, where significant advances have been made during the past half a century in the measurements and modeling of slag properties. Newer experimental techniques and modeling tools have been designed during recent years. The present paper reviews the advances made at the Royal Institute of Technology (KTH), Stockholm during the past two decades.

## 2. Investigations of the Thermodynamic Properties of Slags

### 2.1. Thermodynamic Activities of Slag Components

In the field of thermochemical measurements and modeling, the work was started with the measurement of the activities of FeO in ternary system CaO–FeO–SiO<sub>2</sub> by the galvanic cell method. These measurements were intended as a validation of the technique employed at the Royal Institute of Technology by comparing the results obtained with those earlier reported by Professor Iwase and his group in Kyoto<sup>1)</sup> as well as Wanibe *et al.*<sup>2)</sup> These authors employed the solid electrolyte galvanic cell technique to measure the thermodynamic activity of FeO in the ternary slag as functions of temperature and composition. A typical comparison of our results<sup>3)</sup> is presented in **Fig. 1**.

The figure shows a comparison between the EMF values obtained by the same technique. Only the compositions that are close to each other in the three measurements have been taken up for comparison in this figure. The thermodynamic activity of FeO could be calculated from the EMF values reported. It is to be noted that Wanibe *et al.*<sup>2)</sup> employed air as the reference electrode. In Fig. 1 their values are recalculated for Mo–MoO<sub>2</sub> reference electrode used in our work as well as by Iwase and co-workers.<sup>1)</sup> This was when the inception for the KTH-model for thermodynamic properties was made. The model was based on Temkin description<sup>4)</sup> of ion-

\* Corresponding author: E-mail: raman@kth.se

DOI: <http://dx.doi.org/10.2355/isijinternational.53.1>

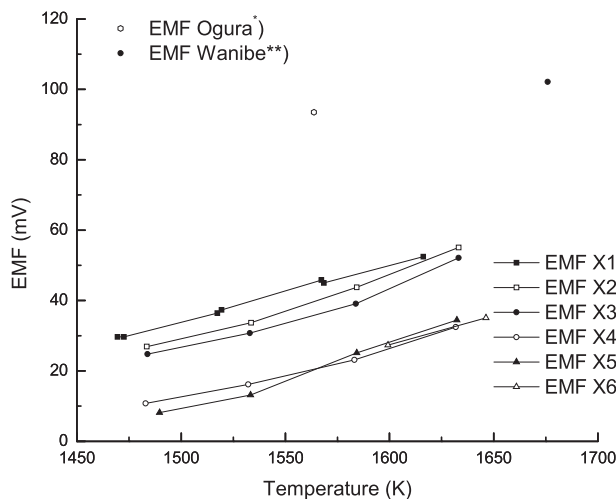


**Fig. 1.** The Results of the EMF measurements at KTH<sup>3)</sup> in the case of CaO–FeO–SiO<sub>2</sub> slags compared with those reported by Ogura *et al.*<sup>1)</sup> and Wanibe *et al.*<sup>2)</sup> Slag compositions are given in wt%: for CaO and FeO. The rest is SiO<sub>2</sub>. X1: CaO=10, FeO=45; X2: CaO=025, FeO=045; X3: CaO=10, FeO=60; X4: CaO=16.5, FeO=46.5; X5: CaO=16.5, FeO=51.5; X6: CaO=11.5, FeO=51.5.

ized melts combining with Lumsden's model<sup>5)</sup> where in silicate ions are considered as being split into Si<sup>4+</sup> and O<sup>2-</sup> ions. The mixing process was based on the Regular Solution concept. The ionic solution can be represented as consisting of cation and anion subgroupings:

$$(A, B, C, \dots)_p (O)_q \dots \dots \dots (1)$$

where A, B, C... represent different cations, O, the oxygen ion and subscripts p and q representing the stoichiometric coefficients. The values of p and q vary with composition maintaining electrical neutrality. The composition is represented by ionic fractions,  $y_i$ . The integral molar Gibbs energy of the ionic liquid is represented by the expression for a pseudo-regular solution as follows:

$$G_m = \sum \sum x_{ij} G_{ij}^o + RT \left[ P \sum (y_i \ln y_i) + Q \sum (y_j \ln y_j) \right] + G^E \dots \dots \dots (2)$$

where  $G_{ij}^o$  represents the standard Gibbs energy of the pure ionic liquid, the second term represents the ideal entropy of mixing for the cations and anions and the term  $G^E$  stands for integral molar Excess Gibbs Energy. This approach was easier compared to some of the rigorous models as it does not consider the type and population of different silicate species in the slag, which would vary with composition, type of cation and temperature.

The thermodynamics of a number of binary and higher order systems<sup>6–12)</sup> were assessed and the values were optimized to mutual consistency. This led to the evolution of the thermodynamic software, Thermoslag, developed in collaboration with the University of Science and Technology Beijing. The software has presently been upgraded in 2012. A typical screen shot of the software with its potentialities is shown in **Fig. 2**.

This module has the capability of computing the activities in a six-component slag system CaO–MgO–MnO–FeO–Al<sub>2</sub>O<sub>3</sub>–SiO<sub>2</sub>. The iso-activity curves for the ternary system CaO–FeO–SiO<sub>2</sub>, drawn according to this model is presented

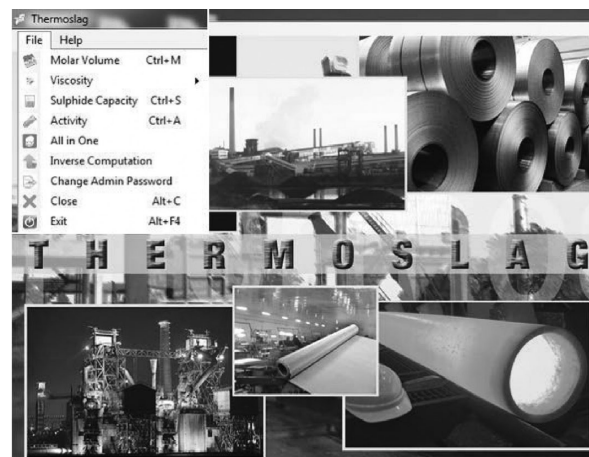


**Fig. 2.** A screen shot from the up-grade version of Thermoslag software.

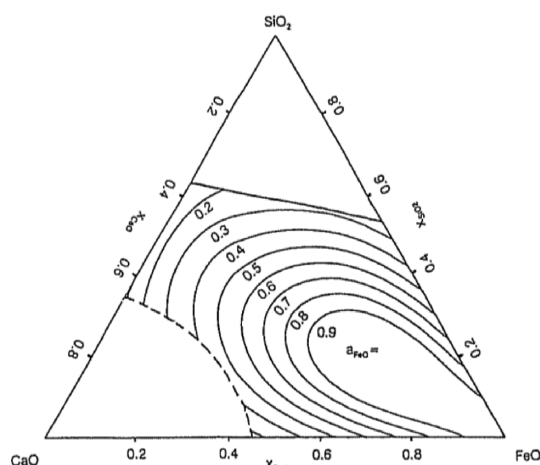


**Fig. 3.** A screen shot of the iso-activity curves predicted by KTH-model for the ternary system CaO–FeO–SiO<sub>2</sub> at 1873 K from the up-graded Thermoslag software for activity calculations.

in **Fig. 3**.

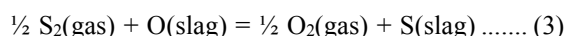
The software is extremely user-friendly and is used by a number of steel industries around the world. Further work has been carried out in determining the activities of CrO and VO<sub>1.5</sub> in slags.<sup>13,14)</sup> In our recent work, the activities of ferrous and ferric oxides could also be measured.<sup>15,16)</sup>

## 2.2. Slag Capacities and Partition Ratios

### 2.2.1. Slag Capacities

One of the industrially important property of slags is the slag capacity, especially the sulphide capacity. This concept was originally presented by Richardson and Fincham.<sup>17)</sup> In order to model sulphide capacities, it is important to have a consistent set of experimental data. The Division of Materials Process Science carried out a systematic investigation of the sulphide capacities of binary, ternary and multicomponent systems involving six components, *viz.* CaO–MgO–MnO–FeO–Al<sub>2</sub>O<sub>3</sub>–SiO<sub>2</sub>. Some of the important publications are referred to here.<sup>18–22)</sup>

Based on these experimental data, the thermodynamic model mentioned under the section on activities was extended to sulphide capacities. The equation adopted was based on the gas-slag equilibrium



viz.

$$C_s = \exp\left(\frac{-\Delta G^\circ}{RT}\right) \left(\frac{a_{\text{O}^{2-}}}{f_{\text{S}^{2-}}}\right) = \exp\left(\frac{-\Delta G^\circ}{RT}\right) \exp\left(-\frac{\xi}{RT}\right) \dots (4)$$

where  $C_s$  is the sulphide capacity of the slag,  $\Delta G^\circ$  is the Gibbs energy change corresponding to reaction (3),  $a_{\text{O}^{2-}}$  is the activity of oxygen ions,  $f_{\text{S}^{2-}}$  is the activity coefficient of sulphide ions,  $R$  is the gas constant,  $T$  the temperature and  $\xi$  is defined by the equation:

$$\left(\frac{a_{\text{O}^{2-}}}{f_{\text{S}^{2-}}}\right) = \exp\left(-\frac{\xi}{RT}\right) \dots\dots\dots (5)$$

This was incorporated into the Thermoslag software mentioned earlier. A screen shot of the iso- $C_s$  curves computed by the sulphide capacity module of the up-graded Thermo-slag software is presented in **Fig. 4**.

A screen shot from the up-graded software showing the variation of sulphide capacity with temperature in the case of the six-component slag  $\text{CaO-MgO-MnO-FeO-Al}_2\text{O}_3\text{-SiO}_2$  is presented in **Fig. 5**.

Some of the very recent advances are the accurate sulphide capacity data generated with relevance to hot metal desulphurization by Taniguchi *et al.*<sup>23,24</sup> Another important mile stone is the sulphide capacity measurements of slags containing  $\text{CrO}_x$ .<sup>25</sup> The novelty of this work was the deduction of structural aspects from these measurements and the evolution of a new concept of basicity of slags.<sup>26</sup>

## 2.2.2. Phosphorus Partition

Phosphorus partition between steel melts and slags with reference to the BOF process was examined in the Division of Materials Process Science. The slags were saturated with  $\text{MgO}$  and crucibles of  $\text{MgO}$  were used. The range of partition studies was widened both with respect to basicity as

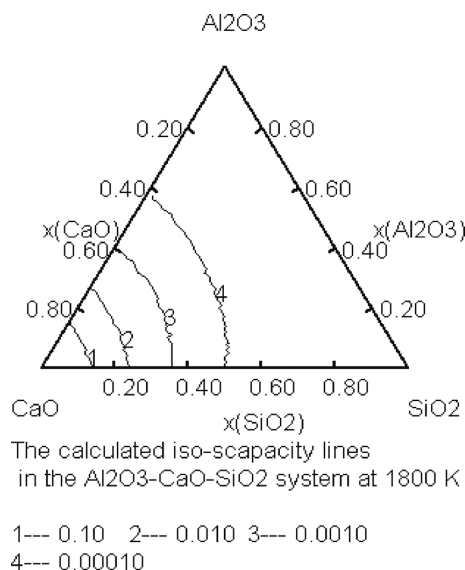


**Fig. 4.** A screen shot of the Thermoslag software for sulphide calculations and Iso- $C_s$  curves predicted by KTH-model for the ternary system  $\text{CaO-Al}_2\text{O}_3\text{-SiO}_2$  at 1800 K.

well as  $\text{FeO}$  content of the slag. Extreme care was taken in the chemical analysis of phosphorus. The results are shown in **Fig. 6**.

The results clearly show that, at a basicity (defined as  $\text{CaO/SiO}_2$ ) of about 2.5, optimum partition is reached. On the other hand, with regard to the  $\text{FeO}$  content, a maximum was reached in the range 15–20 mass%. Thermodynamic correlations were established and with the aid of these, it was shown that the results obtained are in good agreement with those of the earlier researchers, especially Suito *et al.*<sup>29</sup>

## 2.3. Valence States of Cr and V in Slags

One of the interesting experimentation carried out in the Division of Materials Process Science, KTH was on the valence states of chromium by XANES as well as Knudsen cell mass spectrometry measurements.<sup>30</sup> This was the first time that mass spectrometric results were used for evaluating the valence ratio  $\text{Cr}^{2+}/\text{Cr}^{3+}$ . **Figure 7** presents the results wherein the  $\text{Cr}^{2+}/\text{Cr}^{3+}$  ratio (taking into account the effects of temperature and oxygen partial pressure in the term in the Y-axis) is plotted as a function of basicity.

It is seen that these values agree well with those reported earlier in literature. It is also seen that, beyond a critical value of basicity, the valence ratio does not change significantly with basicity. Similar measurements have also been carried out in the case of the valence states of vanadium in metallurgical slags.<sup>31</sup>

## 2.4. Diffusivity of Sulphide Ions in Slags

Diffusivities of various species in slags is an important

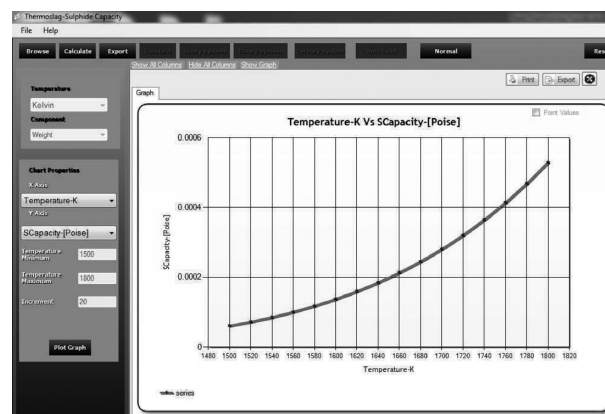


**Fig. 5.** The variation of the sulphide capacity of a  $\text{CaO-MgO-MnO-FeO-Al}_2\text{O}_3\text{-SiO}_2$  slag with temperature.

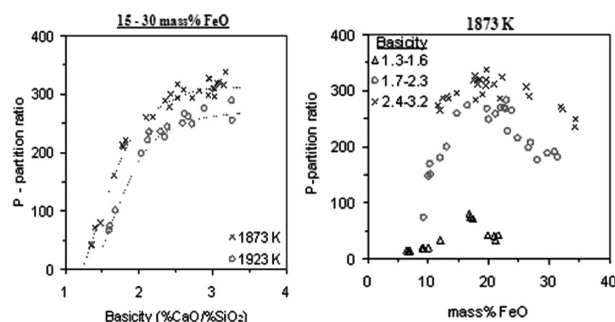


**Fig. 6.** The results of the phosphorus partition ratio investigations.<sup>27,28</sup>

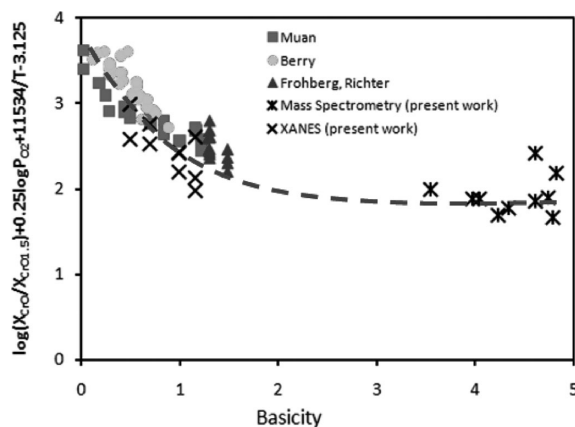


Fig. 7. The ratio ( $\text{Cr}^{2+}/\text{Cr}^{3+}$ ) corrected for the effects of oxygen partial pressure on the Y-axis as a function of basicity defined as  $(\text{CaO} + \text{MgO})/(\text{Al}_2\text{O}_3 + \text{SiO}_2)$ .

parameter with respect to steel refining. At the same time, chemical diffusivities are extremely difficult to measure. Tracer diffusivities have earlier been measured with special reference to the classical work of Saito and Kawai.<sup>32)</sup> A novel method was developed by the present group to measure the chemical diffusivities of sulphur in  $\text{CaO-Al}_2\text{O}_3\text{-SiO}_2$  slags.<sup>33,34)</sup> This arrangement could be successfully used to carry out accurate and reliable measurements of the transport of sulphur diffusing through the slag phase from a defined sulphur potential at the top of the slag phase. After a thorough investigation of the suitable material for the crucible, a crucible made of high-purity iron was used for the diffusivity measurement. The crucible design is presented in Fig. 8(a). The shape of the iron crucible used was designed to facilitate metal sampling without disturbing the slag phase and hence preventing any error because of possible mixing during sampling. The central iron tube had connecting holes at the bottom to the outer crucible. Silver metal with an approximate mass of 350 g was loaded into the iron crucible and was reduced in hydrogen atmosphere at a maximum temperature of 1273 K (1000°C). Silver in the molten state filled both sides of the central tube above the level of the connecting holes. Later, roughly 31 g of slag was loaded in the outer iron crucible. The mass of the slag taken was calculated to have a molten height of approximately 1 cm at the experimental temperature. CaS pellets, dried at 373 K (100°C) were hung above the slag using a Pt wire loop and were lowered after the achievement of thermal equilibrium. The partial pressures of oxygen and sulfur were maintained below  $10^{-7}$  and  $10^{-1}$  Pa, respectively to prevent any possible formation of FeO and FeS. During the experiment, sampling of silver metal was carried out at definite time intervals from the central tube taking precautions so that the slag layer in the outer crucible is not disturbed.

A mathematical model was developed that enabled the calculation of the concentration of sulphur in the silver phase, with the reported diffusivities of sulphide ions by Saito and Kawai as the start values and was optimized further. The optimized sulphur content in liquid Ag and the experimental results are presented in Fig. 8(b).

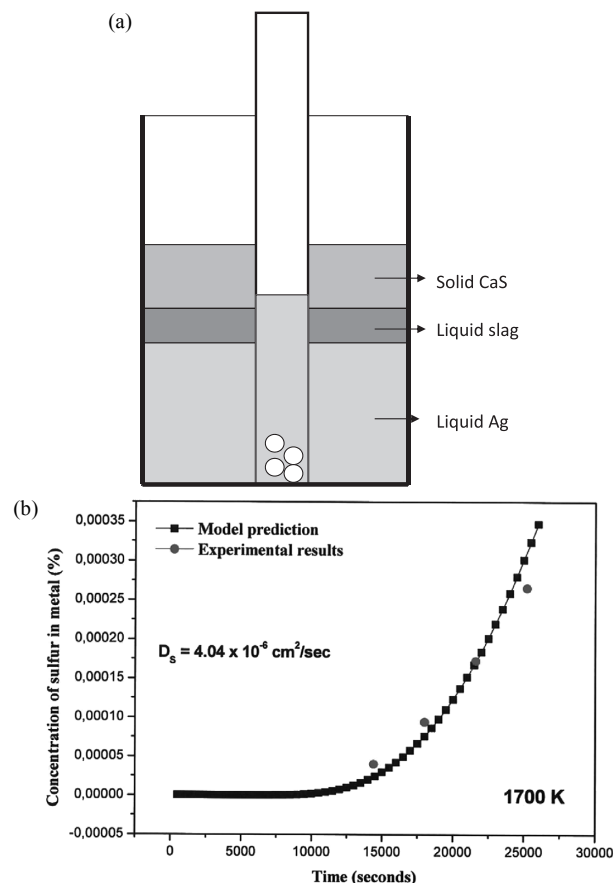


Fig. 8. Measurements of the diffusivity of  $\text{S}^{2-}$  in slags. (a) The specially designed ARMCO iron crucible with a central tube for sampling and (b) the model results on sulphur accumulation in liq. Ag compared with the experimental results.

### 3. Thermophysical Properties of Slags

In the modeling of mass and heat transfer in metallurgical processes, it is important to have access to consistent data on the thermophysical properties of slags. Towards this objective, efforts were concentrated on four thermophysical properties, viz. density (molar volume), viscosity, interfacial tension as well as thermal diffusivity.

#### 3.1. Density/Molar Volume of Slags

Reliable and accurate density measurements are essential in order to develop suitable extrapolations models for densities of slags, needed for process simulations. Two methods were used by the present group for density measurements, viz. Archimedes method and the X-ray sessile-drop method.

In the case of the Archimedes method, which was applied to  $\text{CaO-Al}_2\text{O}_3\text{-SiO}_2$  slags at low silica contents, a platinum 30% rhodium bob was immersed in the slag. The mass changes were followed using an electronic balance. The experimental details are described elsewhere.<sup>35)</sup> The densities could be determined accurately and were found to be in agreement with literature data. The measurements were extended to higher temperatures by the X-ray sessile drop method.<sup>36)</sup> The values were found to be mutually compatible. One interesting feature was that it could be extrapolated to estimate the density of pure, super-cooled CaO, which could be used to optimize the model for densities.

The up-graded Thermoslag software has the module to

calculate the densities/molar volumes of slags with six components CaO–MgO–MnO–FeO–Al<sub>2</sub>O<sub>3</sub>–SiO<sub>2</sub>. A screen shot from the molar volume module of the Thermoslag software is presented in Fig. 9.

### 3.2. Viscosities of Slags

While there are models available to estimate the viscosities of slags, the need for self-consistent data on slag viscosities was lacking. The data generated have to be supported by high temperature calibration of the measurement system. Pre- as well as post measurement analyses of the slag compositions had to be carried out. The slag viscosities were measured by the present group in the case of a number of binary, ternary, quaternary, quinary and six component slags.<sup>37)</sup> The viscosities of CaF<sub>2</sub>-containing slags were also measured.<sup>38)</sup> These values are incorporated in a thermodynamic model for estimating the viscosities of multicomponent slags.<sup>39)</sup> The model is based on Eyring equations and incorporates slag densities and Arrhenius expression of the activation energy for viscous flow.

$$\eta = \frac{hN\rho}{M} \exp\left(\frac{\Delta G^*}{RT}\right) \dots\dots\dots (6)$$

where “ $\eta$ ” is the viscosity, “ $N$ ” is the Avogadro number, “ $h$ ” is the Planck’s constant, “ $\rho$ ” is the density, “ $M$ ” is the molar mass, “ $R$ ” is the gas constant, “ $T$ ” is the absolute temperature and “ $\Delta G^*$ ” is the activation energy for viscous flow. For multicomponent systems, the  $\Delta G^*$  term can be formulated in analogy with Gibbs free energy in thermodynamics, viz.

$$\Delta G^* = \sum_{i=1}^m X_i \Delta G_i^* + \Delta G_{Mix}^* \dots\dots\dots (7)$$

The model has reasonable success in estimating the viscosities of multicomponent slags.<sup>40)</sup> The model along with a database for viscosities has been incorporated into a software, Thermoslag. In the updated version,<sup>41)</sup> the density model is used as a sub-routine to the viscosity calculations so that the two properties are made compatible with each other. The model was extended to CaF<sub>2</sub>-containing slags, making the total number of components in the slag to be 7. A typical viscosity output from the software for a 7-component slag is presented in Fig. 10.

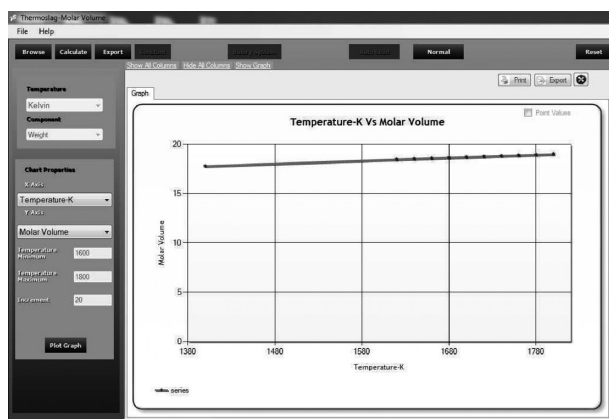


Fig. 9. A screen shot from the density/molar volume of the Thermoslag software for a six-component (CaO–MgO–MnO–FeO–Al<sub>2</sub>O<sub>3</sub>–SiO<sub>2</sub>) slag.

### 3.3. Surface and Interfacial Tension Measurements

The values of surface and interfacial tensions are extremely important for steel refining. The division has an X-ray sessile drop equipment with provision for mixing at least four gases to achieve desired oxygen and sulphur partial pressures in the gas phase. The software for analyzing the drop shape was obtained from Carnegie Mellon University and the image analysis software was developed at the division itself. A milestone among the measurements was the recent studies on the slag metal interactions at the division,<sup>42)</sup> as part of which a new software for the image analysis was developed. The work involved the interfacial tension measurements relevant to hot metal desulphurization process involving Fe–C (liquid), slag (liquid) and solid CaO substrate.

### 3.4. Thermal Diffusivity Measurements

Heat transfer modeling requires reliable values of thermal diffusivities. The division of Materials Process Science has acquired a Sinku-Riko Laser flash unit which could be used for the measurements of thermal diffusivities of slags, sandwiched between two Pt crucibles. A three-layer analysis method combined with differential measurements using two different sample depths were used to evaluate the thermal diffusivities. The method was used to study the thermal diffusivities of CaO–Al<sub>2</sub>O<sub>3</sub>–SiO<sub>2</sub> slags.<sup>43)</sup> An important contribution to an understanding of the thermal diffusivities of mould flux slags, which have a strong impact on the heat transfer in continuous casting moulds was carried out by Hayashi *et al.*<sup>44)</sup> Some of the results are presented in Fig. 11.

This work clearly demonstrated the effect of crystallinity on the thermal diffusivity of these frozen slags. It also clearly demonstrated the absence of the effect of temperature on the thermal diffusivity of mould flux slags in the liquid state.

## 4. Inter-property Correlations

Since the slag properties are structure-based, there should be a natural link between the various properties. Establishment of inter-property correlations enables

- Estimation of properties that are difficult to measure from easily measured other properties,
- There will be a mutual compatibility between properties.

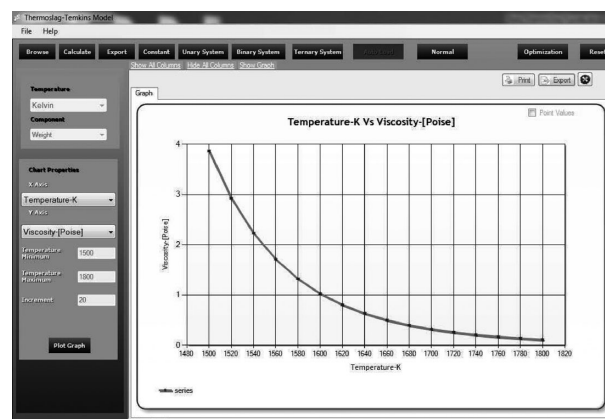
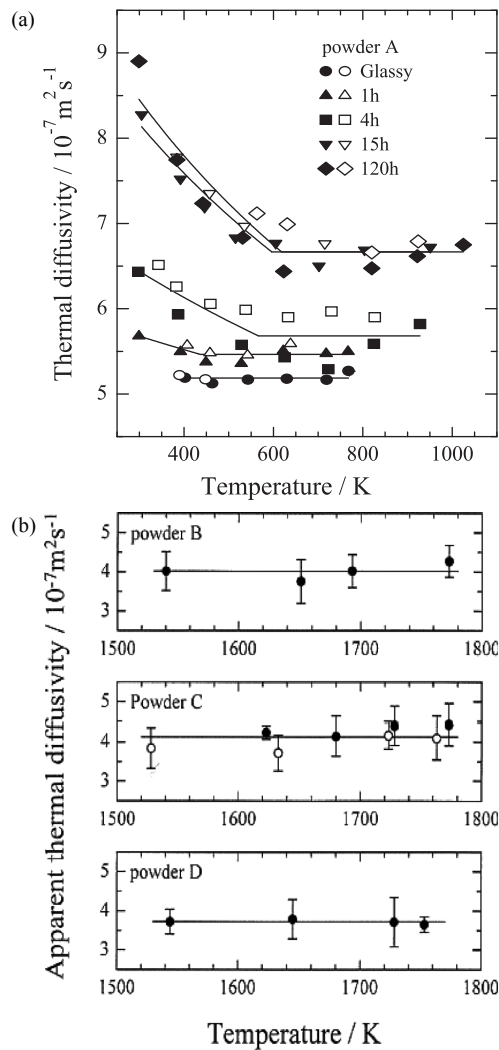


Fig. 10. Viscosity of CaO–MgO–MnO–FeO–Al<sub>2</sub>O<sub>3</sub>–SiO<sub>2</sub>–CaF<sub>2</sub> slags as a function of temperature.





**Fig. 11.** Thermal diffusivities of mould flux slags (a): solid state measurements and (b) liquid state measurements (the latter for different commercial flux powders).

Towards this aim, attempts were made in the present division to establish inter-property correlations. It was possible to establish correlations between the activation energies for viscosities and thermodynamic Gibbs energies of mixing in the case of multicomponent slags,<sup>45)</sup> using Richardson's theory of ideal mixing. The predicted iso-viscosity contours are compared with experimental values in the case of the system CaO–FeO–SiO<sub>2</sub> at 1723 K in **Fig. 12**.

The second derivative approach proposed by Darken<sup>46)</sup> was also utilized in examining the variation of Arrhenius activation energy for viscous flow as a function of temperature. The method opened up a new possibility to estimate the liquidus temperature from viscosity measurements in the case of slags.<sup>47)</sup>

The expression for the second derivative of the activation energy with respect to temperature would be

$$\frac{1}{R} \frac{\partial^2 Q}{\partial T^2} = \frac{\partial^2 \left( \frac{\partial \ln \eta}{\partial \left( \frac{1}{T} \right)} \right)}{\partial T^2} \dots \dots \dots (8)$$

The first and second derivatives of the activation energies in the case of water with respect to temperature are presented

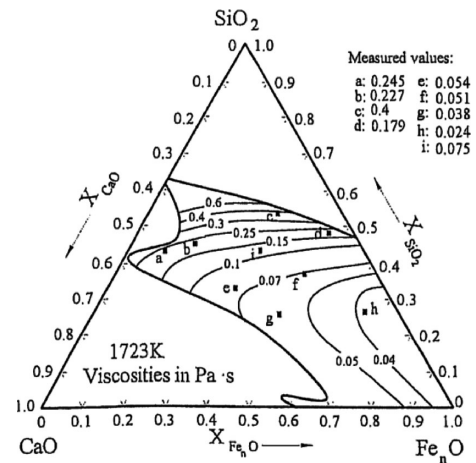


**Fig. 12.** The iso-viscosity contours in the case of the system CaO–FeO–SiO<sub>2</sub> at 1723 K by thermodynamic correlation.<sup>45)</sup>

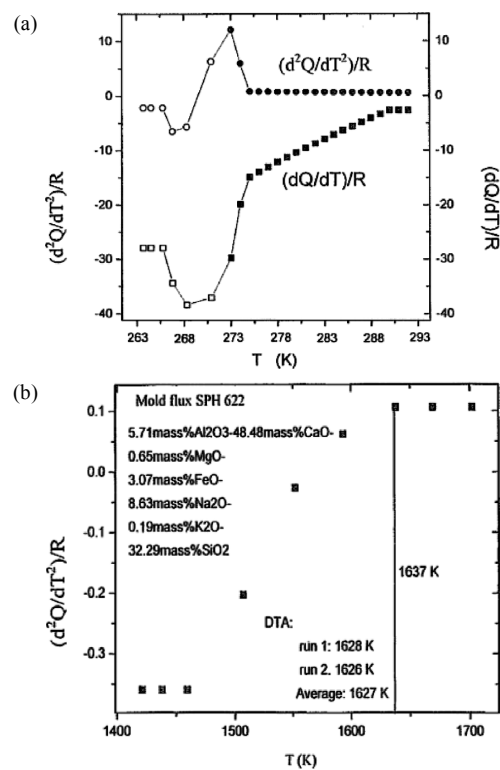


**Fig. 13.** The second derivative approach as applied to (a) water and (b) a commercial mould flux in estimating the liquidus temperatures.

in **Fig. 13(a)**. The values of the activation energies for water correspond to single liquid phase (super-cooled liquid below the freezing point). It is seen that a “break point” occurs at a temperature corresponding to the freezing point of water. This clearly indicates the non-random thermal agitation in the melt just before solidification, indicating the “maturity” of the liquid to produce the solid phase.

This concept can be extended to multi-component slags so that the liquidus temperature of these slags can be estimated from viscosity measurements. Figure 13(b) shows the estimation of the liquidus temperature of a commercial mould flux from the experimental data obtained at our laboratory in the Royal Institute of Technology.

Correlations were also established between integral molar

**Table 1.** Densities of some typical slags from iron and steelmaking.<sup>49)</sup>

Oxide wt-%	BF	EAF	LF
Al <sub>2</sub> O <sub>3</sub>	13	10	33.5
CaO	32	40	53.5
FeO	2	15	0.6
MgO	17	9	6
MnO	2	5	0.4
SiO <sub>2</sub>	34	21	6
Density at 1 873 K [g/cm <sup>3</sup> ]	2.70	2.98	2.67
Molar volume at 1 873 K [cm <sup>3</sup> /mol]	21.2	20.2	24.2

enthalpies of mixing and densities of slags<sup>48,49)</sup> in the case slags involving six components, viz. CaO–MgO–MnO–FeO–Al<sub>2</sub>O<sub>3</sub>–SiO<sub>2</sub>. A typical result in the case of slags in iron and steel processes is presented in Table 1.

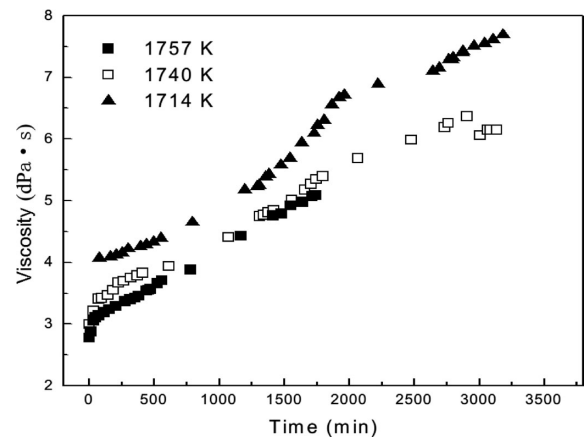
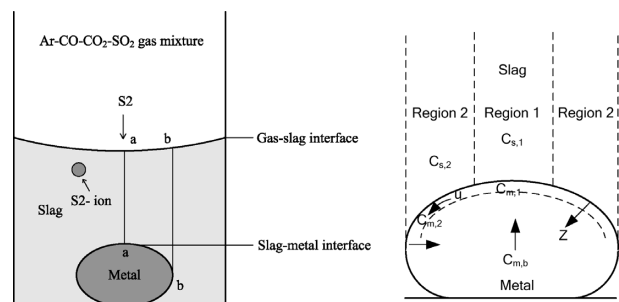
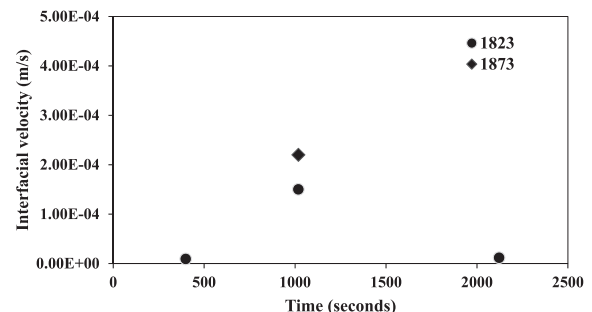
## 5. Dynamic Measurements of Slag Properties

Monitoring the changing of thermophysical properties during a process is expected to provide an insight into the process mechanism. Properties could be used as an index of kinetic reaction rate if the slag structure relaxation is faster than the chemical reaction or the mass transfer step. Under such a condition, the change in the properties during the transition between two states could reflect the rate–controlling step, as for example if it is a chemical reaction or a diffusion mechanism. In such an experimental study, care should be taken so that the change of the property and the response time should be faster than the rate-controlling step of the reaction. In some experimental design, as for example, if a reaction is monitored by following the viscosity changes by the rotating bob method, the measurement would involve forced convection due to the rotation of the bob, which would lead to a faster mass transfer. One of the interesting case studies was the oxidation of fayalite with magnetite precipitation in the slag by following the viscosity changes with time in an oxidizing atmosphere.<sup>50)</sup> Experiments were also conducted to follow the dissolution of Al<sub>2</sub>O<sub>3</sub> in a typical mould flux slag by following the viscosity increase due to alumina dissolution.<sup>51)</sup>

In the case of refractory reactions with molten steel containing oxygen, dynamic contact angle measurements showed a strong evidence of hercynite getting formed at the interface creating non-wetting conditions.<sup>52)</sup> Similar studies have been performed with silica substrate where a fayalite slag was formed<sup>53)</sup> and even mullite substrate.<sup>54)</sup>

Slag foaming is a dynamic phenomenon. A relationship for the foaming index could be derived from film drainage mechanism.<sup>55)</sup> Interesting studies on slag foaming under dynamic conditions were carried out in the present group.<sup>56,57)</sup> These investigations showed that, under dynamic conditions wherein chemical reactions occur in or with the slag phase, the mismatch between the gas generation rate and the gas escape rate causes fluctuations in the foaming of slags.

One of the recent works on the interfacial studies of slag/metal reactions could enable the measurement of interfacial velocities of sulphur at the slag/molten iron interface. The


**Fig. 14.** Dynamic viscosity measurements monitoring the dissolution of alumina in a mould flux slag.<sup>51)</sup>

**Fig. 15.** The X-ray sessile drop arrangement for the study of interfacial velocity of sulphur on the surface of an iron drop immersed in a liquid slag.<sup>58)</sup>

**Fig. 16.** Interfacial velocity of sulphur on iron surface immersed in molten slag.<sup>58)</sup>

experimental arrangement<sup>58)</sup> is presented in Fig. 15.

In this arrangement, well-defined oxygen and sulphur potentials were imposed on the slag surface. With the slight difference in the time sulphur takes to reach different parts of the metal drop surface, the metal drop oscillates due to the Marangoni flow of sulphur along the surface. From the oscillations, which were monitored by X-ray radiography, the surface velocity of sulphur was computed.<sup>58)</sup> The results are shown in Fig. 16.

The effect of oxygen potential on the interfacial velocity of sulphur was measured and it was found that higher oxygen potentials lead to a higher interfacial velocity of sulphur.<sup>59)</sup> The measurements were also extended to oxygen movement along iron surface immersed in a slag phase.<sup>60)</sup>

## 6. Concluding Remarks

An understanding of the properties of slags is of extreme importance for the optimization of metallurgical process. It also enables us to understand the structure of slags. Accurate experimentation is imperative in generating reliable values of thermochemical and thermophysical properties of slags. It is also necessary to develop suitable extrapolation models for the various properties. It is very important to establish inter-property correlations so that the values are mutually compatible and can be used in the same process model. Dynamic measurements of slag properties would be of great help in understanding the process phenomena. These are illustrated by the work on slags carried out in the Division of Materials Process Science, Royal Institute of Technology.

## Acknowledgements

The authors express their sincere gratitude to the Iron and Steel Society of Japan for providing the opportunity to present this review article, summarizing the results generated over the years at the Division of Materials Process Science, Royal Institute of Technology (KTH), Stockholm, Sweden. The financial support from the Swedish Steel Producers Association (Jernkontoret) for the research in slags over the years is gratefully acknowledged. The authors also express their sincere thanks to the scientists from all over the world who collaborated with us all these years. We thank Mr. Xianfeng Hu for his kind help in preparing this manuscript.

## REFERENCES

- 1) T. Ogura, R. Fujiwara, R. Mochizuki, Y. Kawamoto, T. Oishi and M. Iwase: *Metall. Mater. Trans.*, **23B** (1992), 459.
- 2) Y. Wanibe, Y. Yaauchi, K. Kawai and H. Sakao: *Arch Eisenhüttenwes*, **44** (1973), 711.
- 3) J. Bygdén, D. Sichen and S. Seetharaman: *Steel Res. Int.*, **10** (1994), 421.
- 4) M. Temkin: *Acta Phys. Chem. URSS*, **20** (1945), 411.
- 5) J. Lumsden: *Int. Symp. Physical Chem. of Proc. Metallurgy*, Part I, ed. by G. R. St. Pierre, AIME, Pittsburgh, PA, (1959), 165.
- 6) J. Björkvall, D. Sichen and S. Seetharaman: *High Temp. Mater. Proc.*, **18** (1999), 253.
- 7) J. Björkvall, D. Sichen and S. Seetharaman: *High Temp. Mater. Proc.*, **19** (2000), 49.
- 8) J. Björkvall, D. Sichen and S. Seetharaman: *Calphad*, **24** (2000), 353.
- 9) J. Björkvall, D. Sichen and S. Seetharaman: *Ironmaking Steelmaking*, **28** (2001), 1.
- 10) P. Fredriksson and S. Seetharaman: *Steel Res. Int.*, **75** (2004), 240.
- 11) P. Fredriksson and S. Seetharaman: *Steel Res. Int.*, **75** (2004), 357.
- 12) P. Fredriksson and S. Seetharaman: *Ironmaking Steelmaking*, **32** (2005), 47.
- 13) P. Dong, X. Wang and S. Seetharaman: *Steel Res. Int.*, **80** (2009), 202.
- 14) P. Dong, X. Wang and S. Seetharaman: *Steel Res. Int.*, **80** (2009), 251.
- 15) S. Basu, A. K. Lahiri and S. Seetharaman: *Metall. Mater. Trans.*, **39B** (2008), 447.
- 16) S. Basu, A. K. Lahiri and S. Seetharaman: *Metall. Mater. Trans.*, **41B** (2010), 414.
- 17) F. D. Richardson and C. J. B. Fincham: *J. Iron Steel Inst.*, **178** (1954), 4.
- 18) E. Drakaliyski, R. Nilsson, D. Sichen and S. Seetharaman: *High Temp. Mater. Proc.*, **15** (1996), 263.
- 19) R. Nilsson, D. Sichen and S. Seetharaman: *Scand. J. Metall.*, **26** (1996), 128.
- 20) M. M. Nzotta, D. Sichen and S. Seetharaman: *ISIJ Int.*, **38** (1998), 1170.
- 21) M. M. Nzotta, D. Sichen and S. Seetharaman: *Metall. Mater. Trans.*, **30B** (1999), 909.
- 22) M. M. Nzotta, D. Sichen and S. Seetharaman: *ISIJ Int.*, **39** (1999), 657.
- 23) Y. Taniguchi, L. Wang, N. Sano and S. Seetharaman: *Metall. Mater. Trans. B*, **43B** (2012), 1-3, DOI: 10.1007/s11663-011-962.
- 24) Y. Taniguchi, N. Sano and S. Seetharaman: *ISIJ Int.*, **49** (2009), 156.
- 25) L. J. Wang and S. Seetharaman: *Metall. Mater. Trans. B*, **41B** (2010), 367.
- 26) L. J. Wang, M. Hayashi, K. C. Chou and S. Seetharaman: *Metall. Mater. Trans. B*, (2011), submitted.
- 27) S. Basu, A. K. Lahiri and S. Seetharaman: *Metall. Mater. Trans. B*, **38B** (2007), 357.
- 28) S. Basu, A. K. Lahiri and S. Seetharaman: *Metall. Mater. Trans. B*, **38B** (2007), 623.
- 29) H. Suito, R. Inoue and M. Takada: *Trans. Iron Steel Inst. Jpn.*, **21** (1981), 250.
- 30) L. J. Wang and S. Seetharaman: *Metall. Mater. Trans. B*, **41B** (2010), 946.
- 31) H. J. Wang, L. J. Wang and S. Seetharaman: *Metall. Mater. Trans. B*, (2010), submitted.
- 32) T. Saito and Y. Kawai: *Jpn. J. Inst. Met.*, **17** (1953), 434.
- 33) L. Muhmood, N. N. Viswanathan and S. Seetharaman: *Metall. Mater. Trans.*, **42B** (2011), 393.
- 34) L. Muhmood, N. N. Viswanathan and S. Seetharaman: *Metall. Mater. Trans.*, **42B** (2011), 274.
- 35) L. Muhmood and S. Seetharaman: *Metall. Mater. Trans.*, **41B** (2010), 833.
- 36) L. Muhmood, N. N. Viswanathan and S. Seetharaman: *Metall. Mater. Trans.*, **42B** (2011), 460.
- 37) F. Ji: PhD Thesis, Royal Institute of Technology, Stockholm, Sweden, (1999).
- 38) F. Shahbazian: PhD Thesis, Royal Institute of Technology, Stockholm, Sweden, (2002).
- 39) F. Ji, D. Sichen and S. Seetharaman: *Int. J. Thermophys.*, **20** (1999), 309.
- 40) S. Seetharaman, K. Mukai and S. D. Sichen: *Steel Res. Int.*, **76** (2005), 267.
- 41) Thermoslag Software, updated version, Division of Materials Process Science, Royal Institute of Technology, Stockholm, Sweden, (2012).
- 42) Y. Taniguchi and S. Seetharaman: *Metall. Mater. Trans. B*, **43B** (2012), DOI: 10.1007/s11663-012-9639-1.
- 43) R. Eriksson, M. Hayashi and S. Seetharaman: *Int. J. Thermophys.*, **24** (2003), 785.
- 44) M. Hayashi, R. A. Abas and S. Seetharaman: *ISIJ Int.*, **44** (2004), 691.
- 45) S. Seetharaman, D. Sichen and F. Z. Ji: *Metall. Mater. Trans.*, **31B** (2000), 105.
- 46) L. S. Darken: *Trans. Metall. Soc. AIME*, **239** (1967), 80.
- 47) S. Seetharaman, S. Sridhar, D. Sichen and K. C. Mills: *Metall. Mater. Trans.*, **31B** (2000), 111.
- 48) M. Persson, T. Matsushita, J. Zhang and S. Seetharaman: *Steel Res. Int.*, **78** (2007), 102.
- 49) M. Persson, J. Zhang and S. Seetharaman: *Steel Res. Int.*, **38B** (2007), 290.
- 50) N. N. Viswanathan, F. Z. Ji, D. Sichen and S. Seetharaman: *ISIJ Int.*, **41** (2001), 722.
- 51) F. Shahbazian, D. Sichen and S. Seetharaman: *ISIJ Int.*, **42** (2002), 155.
- 52) E. Kapilashrami, A. Jakobsson, A. K. Lahiri and S. Seetharaman: *Metall. Mater. Trans.*, **34B** (2003), 193.
- 53) E. Kapilashrami, A. K. Lahiri, A. W. Cramb and S. Seetharaman: *Metall. Mater. Trans.*, **34B** (2003), 647.
- 54) E. Kapilashrami, V. Sahajwalla and S. Seetharaman: *ISIJ Int.*, **44** (2004), 653.
- 55) A. K. Lahiri and S. Seetharaman: *Metall. Mater. Trans.*, **33B** (2002), 499.
- 56) A. Kapilashrami, M. Görnerup, A. HK. Lahiri and S. Seetharaman: *Metall. Mater. Trans.*, **37B** (2006), 109.
- 57) A. Kapilashrami, A. K. Lahiri, M. Görnerup and S. Seetharaman: *Metall. Mater. Trans.*, **37B** (2006), 145.
- 58) L. Muhmood, N. N. Viswanathan and S. Seetharaman: *Metall. Mater. Trans.*, **42B** (2011), 460.
- 59) W. Cao, L. Muhmood and S. Seetharaman: *Metall. Mater. Trans.*, **43B** (2012), 363.
- 60) L. Muhmood, N. N. Viswanathan and S. Seetharaman: *Int. J. Mat. Res.*, (2012), e-first issue, DOI: 10.3139/146.110705.